SCIENCE CHINA Materials

LETTERS

mater.scichina.com link.springer.com

Published online 17 April 2018 | https://doi.org/10.1007/s40843-018-9255-9

Sci China Mater 2018, 61(10): 1351–1359

Robust photoluminescence energy of MoS_2/graphene heterostructure against electron irradiation

Shengzhe Hong[1†], Deyi Fu[2†], Jiwei Hou[1], Duanliang Zhou[3], Bolun Wang[1], Yufei Sun[1], Peng Liu[3] and Kai Liu[1*]

Two-dimensional (2D) materials have attracted growing attention since the discovery of graphene [1]. Transition metal dichalcogenide (TMD) semiconductors, such as MoS_2 and WS_2, became popular materials in recent years, because they usually have intrinsic bandgaps and an indirect-to-direct bandgap transition from bulk to monolayer limit [2–6]. Although graphene and TMDs are promising materials in field-effect devices [7–9], their heterostructures are more advanced in charge-splitting functions for the applications in optoelectronic devices [10–15]. In these heterostructure devices, graphene has been utilized as an effective electrode to reduce the contact resistance in 2D semiconductor devices due to its ultra-flat surface, high carrier mobility, and gate-tunable Fermi level. The diversity of 2D semiconductors has also enabled 2D heterostructures with multiple functionalities to meet various demands in applications [16–21].

Modulation of 2D heterostructure properties is desired for their diverse applications. Defect engineering of materials, which can be achieved by irradiation of particles such as electrons or ions, provides an effective way to modulate properties of materials, as proven in silicon industry. Currently, diverse irradiation sources, including argon ions (Ar^+) [22,23], electrons [24–26], helium ions (He^+) [27–29], carbon ions [30] and oxygen plasma [31–33], have been utilized to bombard 2D materials. Irradiation could controllably introduce defects that strongly scatter phonons and electrons limited in the 2D surface, which generally degrades the intrinsic properties of 2D materials including mechanical strength [34], carrier mobility [23] and thermal conductivity [35]. However, abnormal behaviors are also observed, for example, an enhancement in elastic modulus after Ar^+ irradiation in graphene [22], and an improvement in electrical conductivity after a mild oxygen treatment in MoS_2 [32]. It has been shown that upon electron irradiation, 2D TMDs can be modified with vacancy defects and doped by filling the vacancies with impurity atoms [25], and graphene is also doped with electrons or holes depending on the irradiation energy [26]. So far these effects of irradiation have been mostly investigated in single 2D materials. Effects of irradiation on 2D heterostructures have yet to be well explored, and whether the build-up of 2D heterostructures could circumvent the degradation of the materials remains a question.

In this work, we found that the build-up of heterostructures could partly hinder the degradation of the properties of monolayer MoS_2 against electron irradiation damage. By insertion of a monolayer graphene between MoS_2 and the substrate, the photoluminescence (PL) from MoS_2/graphene heterostructure area is always stronger in intensity and more robust in energy under electron irradiation, in contrast to the dramatic PL shift in the MoS_2 monolayer area. The improvement is attributed to a blocking effect of graphene that prevents MoS_2 from being affected by the substrate. Raman spectra and electrical transfer properties were also investigated to systematically reveal the effect of electron irradiation on the MoS_2/graphene heterostructure. Our work not only deepens the understanding of irradiation effects on 2D heterostructures, but also paves the way to the design of novel irradiation-resistant devices.

Electron irradiation exists commonly in environments ranging from materials observation under electron mi-

[1] State Key Laboratory of New Ceramics and Fine Processing, School of Materials Science and Engineering, Tsinghua University, Beijing 100084, China

[2] Department of Physics, National University of Singapore, 2 Science Drive 3, Singapore 117551, Singapore

[3] Department of Physics and Tsinghua-Foxconn Nanotechnology Research Center, Tsinghua University, Beijing 100084, China

† These authors contributed equally to this work.

* Corresponding author (email: liuk@tsinghua.edu.cn)

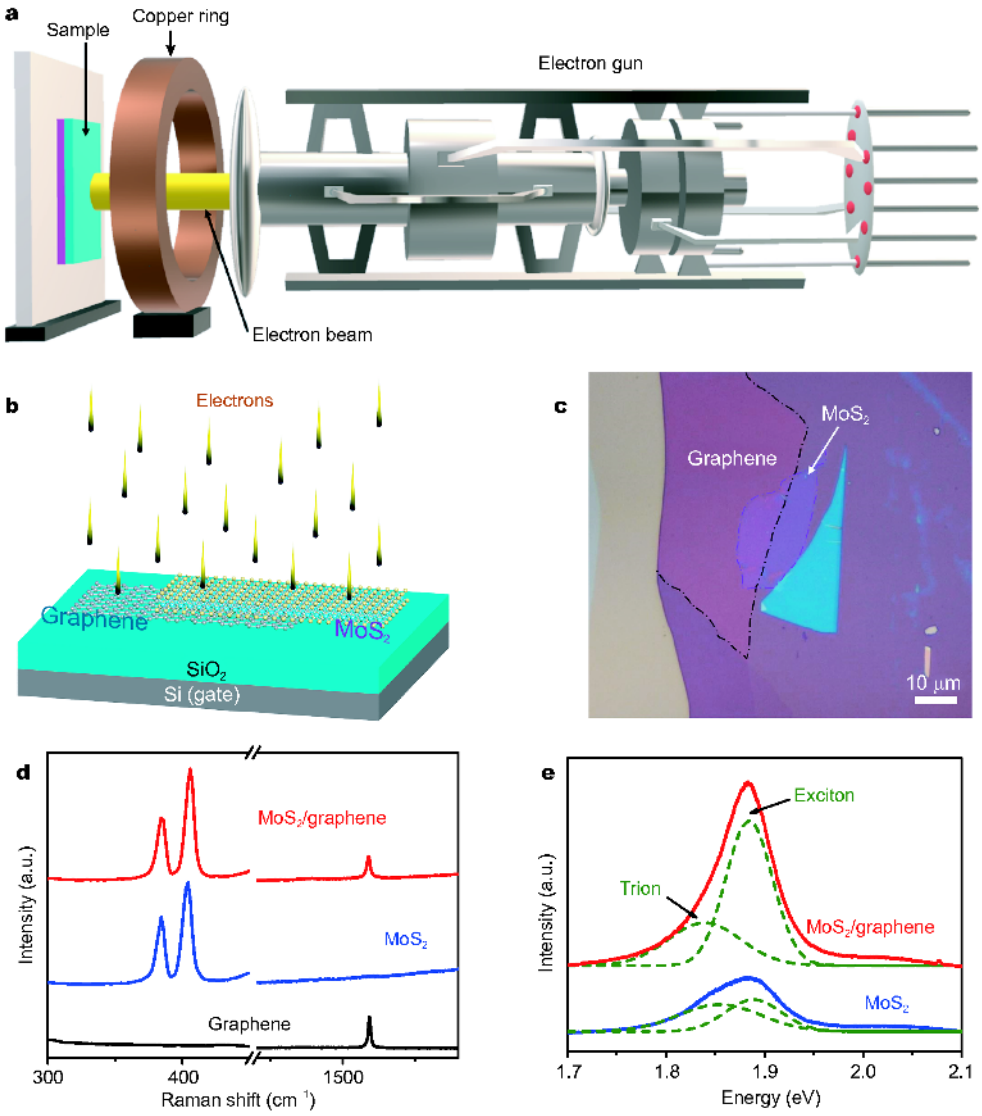

Figure 1 Schematics of electron irradiation and optical properties of pristine samples. (a) Schematic of our homemade electron beam generator. (b) Illustrative diagram of a MoS_2/graphene heterostructure irradiated by electrons. (c) Optical image of a monolayer MoS_2/graphene heterostructure. (d, e) Raman and PL spectra of monolayer MoS_2, graphene, and their heterostructure. The dashed lines indicate peak fittings to the original PL spectra, which can be split into exciton and trion peaks.

croscopy to devices application in space exploration. For 2D devices working in such harsh environments, their resistance to electron irradiation is of vital importance because the ultrathin materials could be easily damaged even under a low dose of irradiation. Compared to other types of irradiation means with heavier particles (e.g., He^+ and Ar^+), electron irradiation provides a more gentle and controllable way to study the effect of irradiation on 2D materials. Scanning electron microscope (SEM) or transmission electron microscope (TEM) have been employed as electron sources to irradiate several 2D materials [24,26,36]. These approaches can work well on tiny samples but will introduce heterogeneity in irradiation dose for large-area samples.

Here we set up a home-made electron source (Fig. 1a) to irradiate our samples. The electron spot spans as large as ~4 mm in diameter such that the monolayer MoS_2 and graphene, and their heterostructure region are irradiated simultaneously and uniformly (Fig. 1b). The MoS_2/graphene heterostructures were fabricated by stacking mechanically exfoliated monolayer MoS_2 onto the top of mechanically exfoliated monolayer graphene (Fig. 1c), or in a reversed order, with a PDMS-assisted transfer process (Supplementary information Fig. S1). We used ex-

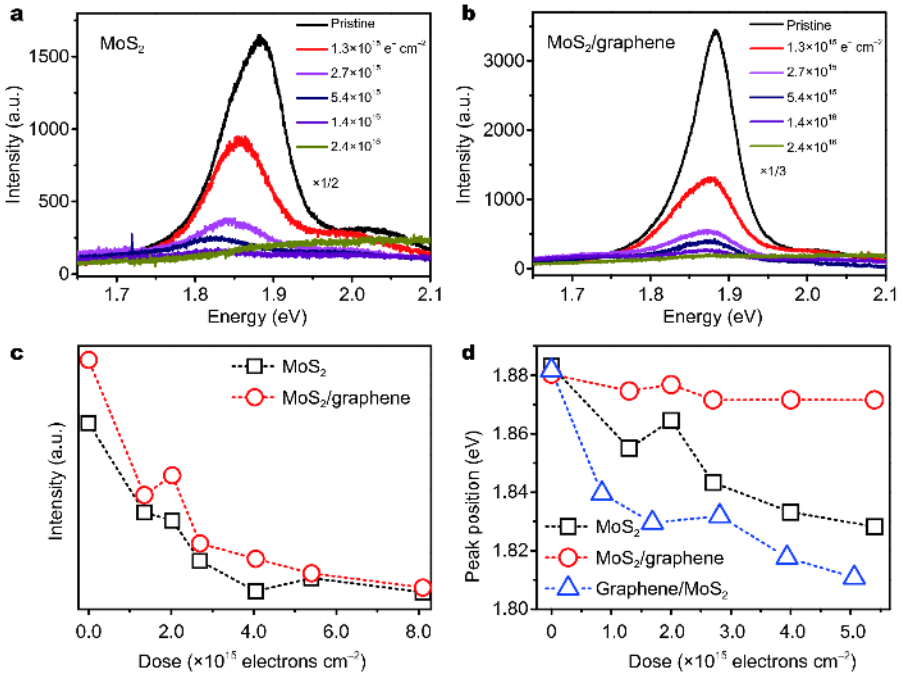

Figure 2 Comparison of PL spectra of monolayer MoS (a) and MoS_2/graphene (b) under electron irradiation. (c) Comparison of PL integral intensity of monolayer MoS_2 and MoS_2/graphene heterostructure under different doses of electron irradiation. (d) Dependence of PL peak positions on the irradiation for bare MoS_2, MoS_2 (top)/graphene (bottom) heterostructure, and graphene (top)/MoS_2 (bottom) heterostructure.

foliated 2D materials in this study as they are intrinsically defect-free or have low defect densities, which are beneficial to study the effect of electron irradiation that usually introduces additional defects in the materials.

As shown in Fig. 1d, the MoS_2/graphene heterostructure has a combined feature of MoS_2 and graphene, including an out-of-plane mode A_{1g} (~405 cm^{-1}) and an in-plane mode E^1_{2g} (~386 cm^{-1}) from MoS_2, as well as a G peak (~1,580 cm^{-1}) from graphene. Compared to monolayer MoS_2, the E^1_{2g} peak of MoS_2/graphene heterostructure remains unchanged while A_{1g} peak blue-shifts by ~2 cm^{-1}. Because the A_{1g} peak is sensitive to the concentration of electrons [37], this phenomenon suggests electron transfer from MoS_2 to graphene exists in the heterostructure. Fig. 1e shows that the PL of the heterostructure has a much stronger intensity than that of the monolayer MoS_2. The PL can be split into two peaks that are dominated by the recombination of excitons (electron-hole pairs, ~1.88 eV) and trions (electron-electron-hole clusters, ~1.84 eV), respectively [38]. In the PL of MoS_2/graphene heterostructure (Fig. 1e, red curve), the larger ratio of exciton to trion contribution further confirms the electron depletion of MoS_2 in the heterostructure, which results from the transfer of electrons from MoS_2 to graphene due to the lower Fermi level of graphene, because the graphene used here is highly p-doped as shown in the electrical measurements (Fig. S2)

Fig. 2 shows the evolution of PL upon electron irradiation for monolayer MoS_2 (Fig. 2a) and MoS_2/graphene heterostructure (Fig. 2b). As expected, both the intensity of MoS_2 and MoS_2/graphene decreases with increasing the irradiation doses (Fig. 2c). However, the PL intensity of MoS_2/graphene is always stronger than that of MoS_2 for the dose up to 8×10^{15} electrons cm^{-2}. The other interesting phenomenon is that the PL peak of the heterostructure remains nearly unchanged under the electron irradiation. The largest PL peak shift is only ~0.01 eV under the highest irradiation dose (1.3×10^{16} electrons cm^{-2}), compared to the non-irradiated MoS_2/graphene (Fig. 2d). In contrast, the PL peak of monolayer MoS_2 red-shifts gradually with increasing the dose of electron irradiation (Fig. 2d), and drops by ~0.06 eV under the irradiation dose of 8.0×10^{15} electrons cm^{-2}, which is six times the value of the heterostructure. It reveals a 'passivation' effect for MoS_2 owing to the insertion of graphene layer between MoS_2 and the substrate, which induces more robust optical property of MoS_2 on the top of graphene against electron irradiation.

Under the 10 keV acceleration voltage, the incident electron beam would irradiate and penetrate through the

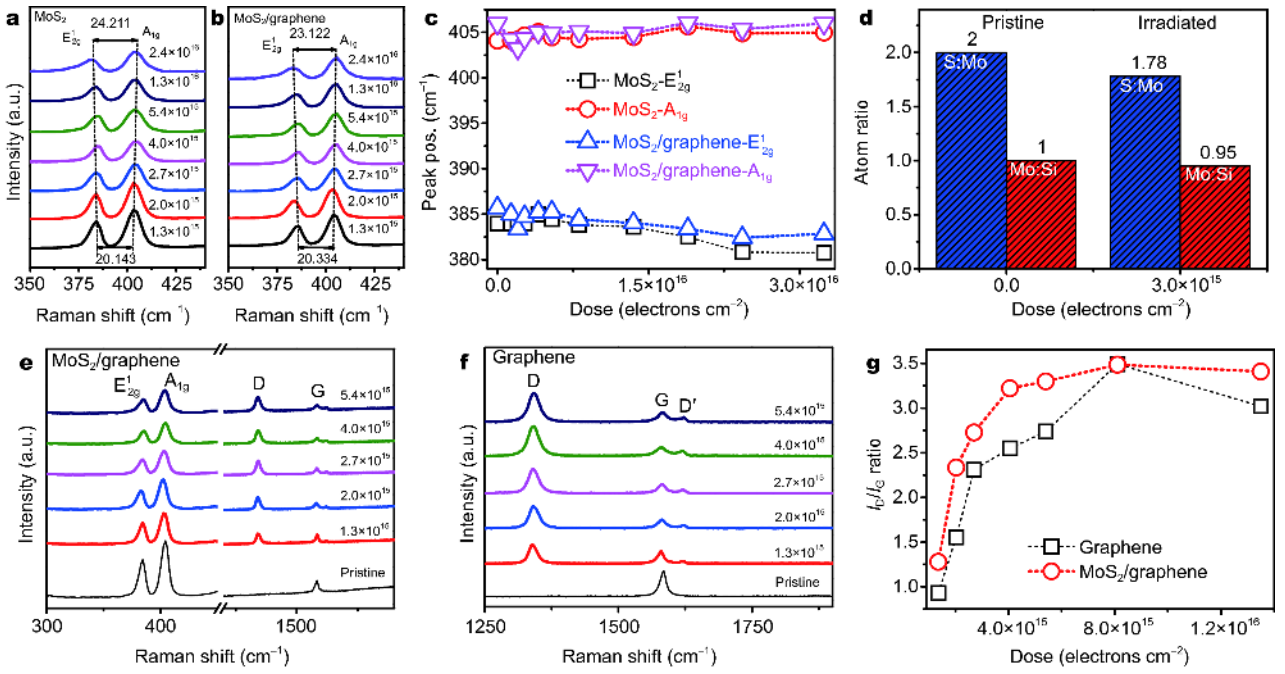

Figure 3 Raman spectra analysis under different electron dose. Raman spectra of (a) monolayer MoS_2 and (b) MoS_2/graphene. (c) The peak position changes of E^1_{2g} and A_{1g} with increasing dose. (d) Atomic ratios of S:Mo and Mo:Si for a pristine MoS_2 and an irradiated sample under the dose of 3×10^{15} electrons cm^{-2}, respectively, which is obtained from X-ray photoelectron spectroscopy (XPS) spectra. The initial ratios of S:Mo and Mo:Si are calibrated to 2 and 1, respectively, for the pristine sample. Raman spectra of (e) MoS_2/graphene and (f) monolayer graphene. (g) Comparison of the ratio between D peak (1,350 cm^{-1}) and G peak (1,580 cm^{-1}) of monolayer graphene and MoS_2/graphene heterostructure.

ultrathin monolayer MoS_2 or bilayer MoS_2/graphene heterostructure, and ultimately inject into the underneath SiO_2/Si substrate [26]. The bombardment of electrons could create structural defects in MoS_2 and graphene. To elucidate the effect of electron irradiation on structural defects of the materials, we adopted Raman spectra and XPS to probe the defects in graphene and MoS_2 (Fig. S3). As shown in Fig. 3a–c, the Raman spectra of monolayer MoS_2 and MoS_2/graphene before and after electron irradiation are compared. Both A_{1g} modes remain nearly unchanged while both E^1_{2g} modes red-shift after irradiation (Fig. 3c). This behavior results in an increase of the separation between E^1_{2g} and A_{1g} peaks by ~4 cm^{-1}, for both monolayer MoS_2 and MoS_2/graphene, when the irradiation does reaches 3.2×10^{16} electrons cm^{-2} (Fig. 3a, b). The full-wide-at-half-maximum (FWHM) for both cases also shows the same trend of broadening. It is known that the A_{1g} mode is related to the doping level and the E^1_{2g} mode is sensitive to lattice distortion (or strain) in MoS_2. The red-shift of E^1_{2g} should result from the softening of lattice due to the vacancy defects induced by electron irradiation. XPS measurements confirm that the defects are mainly S vacancies in irradiated MoS_2 because the S:Mo atomic ratio after irradiation becomes much less than 2 while the Mo:Si ratio remains nearly unchanged (Fig. 3d). The creation of S vacancy is also reported by other particle irradiation approaches including He^+ [27] and Ar^+ irradiation [23,29].

Next we analyzed the Raman peaks of graphene in monolayer region and the heterostructure (Fig. 3e, f). In the pristine monolayer graphene and MoS_2/graphene samples, there is a strong G peak (~1,580 cm^{-1}) while the D peak (~1,350 cm^{-1}), which relates to disorder in carbon lattice [39,40], is hardly observed, suggesting an unnoticeable amount of defects in the pristine samples. As expected, the D peak becomes remarkable and increases in intensity with the increase of irradiation dose due to generation of defects. The intensity ratio of the D to G peak could be used to evaluate the defect intensity in graphene [39], and is also found to be sensitive to the doping level of graphene [41]. Fig. 3g shows that I_D/I_G is relatively higher for MoS_2/graphene than for monolayer graphene under different doses of irradiation, indicating a higher doping level. This phenomenon may result from the electron transfer from MoS_2 to graphene in the heterostructure as aforementioned.

The question is why the PL of MoS_2 on graphene appears more robust in peak position compared to that of

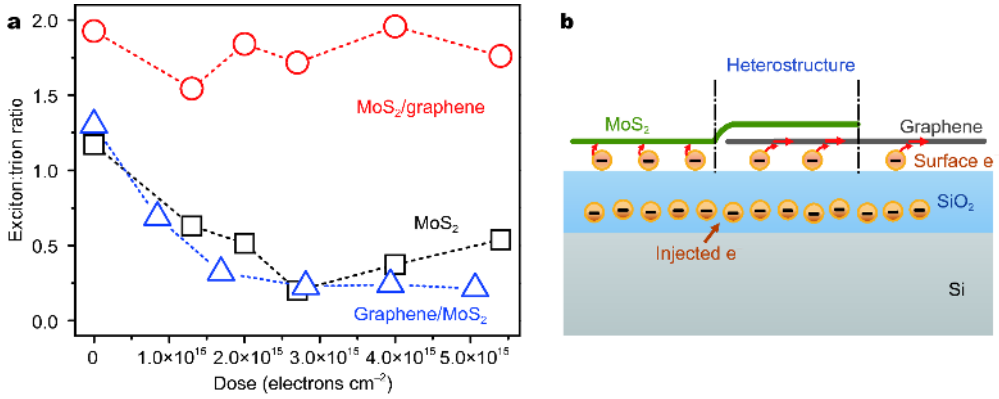

Figure 4 Extrinsic doping of MoS_2 by electron irradiation. (a) The evolution of intensity ratio of exciton:trion for MoS_2, MoS_2/graphene and graphene/MoS_2 with the irradiation dose. (b) Schematic of the charge doping at the substrate interface.

MoS_2. In bare MoS_2, the red-shift of the PL peak (Fig. 2d) and the decreased exciton-to-trion intensity ratio (Fig. 4a) reveal that the MoS_2 should be doped by electrons under irradiation, because additionally doped electrons will drive a transition from exciton- to trion-dominant PL in MoS_2 [38]. However, this effect seems to be suppressed by some way in the heterostructure region, as shown in Figs 2d and 4a.

The doping effect could originate from intrinsic defects [42], molecular adsorbates at defective sites [43], or extrinsic charge doping that arises from a balance of electron injection, emission of secondary electrons, and diffusion of charges in the substrate [26]. H_2O or O_2 molecular are able to adsorb at defects in MoS_2, but they will dope the MoS_2 with holes and blue-shift its PL peak [43], which is opposite to our observation and should not be the dominant mechanism. In contrast, intrinsic structural defects, i.e., sulfur vacancies as shown in Fig. 3d, were reported to induce an n-doping in MoS_2 [42]. In this case, the doped, additional electrons would be transferred to graphene at the MoS_2/graphene heterostructure region, because the work function of graphene is higher than that of MoS_2 (Fig. S2). This picture appears to be able to explain the robust PL peak of MoS_2/graphene.

To further clarify the mechanism, we carried out a control experiment by stacking the heterostructure in a reverse order (i.e., encapsulating MoS_2 with a top graphene layer, namely graphene/MoS_2, Fig. S4). If the doping induced by irradiated defects and the charge transfer between MoS_2 and graphene played the dominant role, a robust PL peak should be also observed in the graphene/MoS_2 geometry. However, experimental results show that both the PL peak of graphene/MoS_2 and its exciton-to-trion intensity ratio decrease with increasing the irradiation dose (Figs 2d and 4a), a phenomenon very similar to bare MoS_2 but in sharp contrast to MoS_2/graphene. Therefore, it reveals that the observed phenomenon strongly depends on the stacking order of the heterostructure.

In both bare MoS_2 and graphene/MoS_2, MoS_2 interacts with the substrate directly, while in MoS_2/graphene, it is separated from the substrate by graphene. This suggests an unnegligible role of the substrate surface, as revealed in most of 2D systems [44–46]. The high-energy electrons will irradiate the 2D layers and finally inject into a depth of SiO_2/Si substrate. The doping of MoS_2 induced by the capacitive charging of injected electrons is negligible because both MoS_2 and graphene are floating in the PL measurements. In addition, the high-energy electrons bombarding onto the surface of SiO_2/Si substrate can generate low-energy secondary electron emission (SEE). These low-energy electrons could be trapped at the 2D layer-substrate interface, causing an n-type doping effect to the contacted 2D layer. When graphene is in between MoS_2 and the substrate, any electrons generated by SEE effect at the substrate interface will be absorbed by the graphene layer, therefore suppressing the n-type doping effect on the top MoS_2 layer (Fig. 4b). As a results, a robust PL peak with dominant exciton luminesce is expected, as shown in Figs 2b and 4a. When graphene is on the top, however, the MoS_2 monolayer directly touches the substrate, and the electrons generated by SEE effect can be easily injected back into the MoS_2 monolayer, leading to an n-type doping effect. As aforementioned, this n-type doing will suppress exciton luminescence and cause red-shift of PL peak when irradiation dose is increased. As a result, the graphene acts not only as a charge

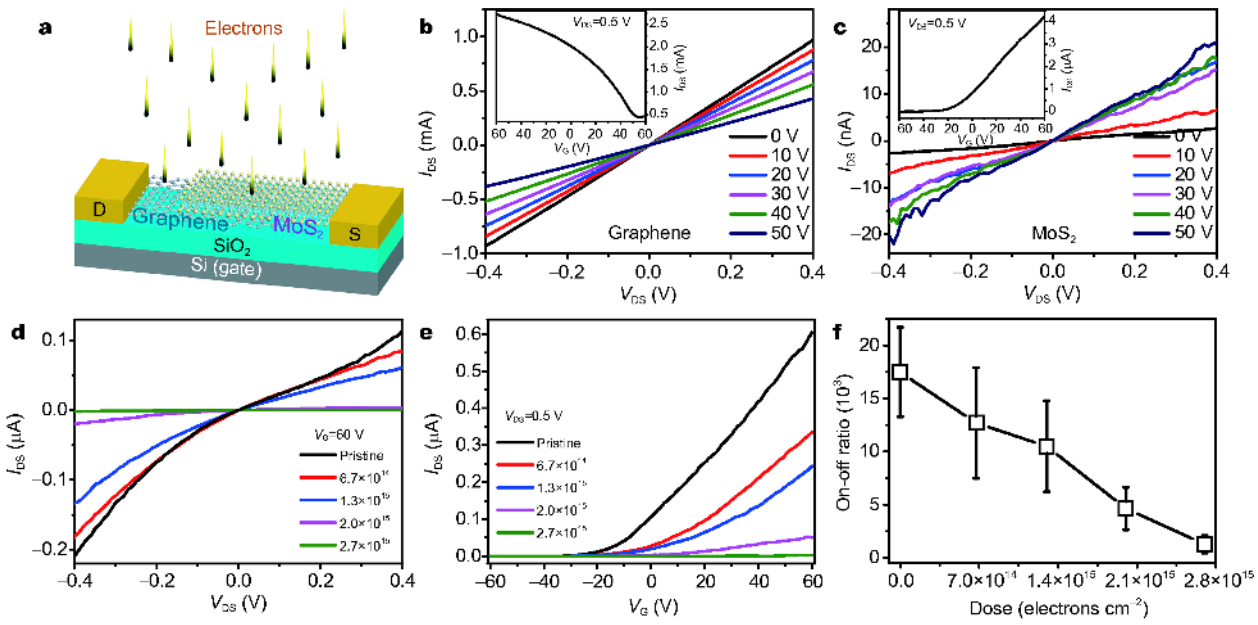

Figure 5 Transport properties of MoS_2/graphene heterostructure under electron irradiation. (a) Schematic of a MoS_2/graphene FET under irradiation. (b) I_{DS}-V_{DS} characteristics of monolayer graphene at different back gate biases. Inset: transfer curve of graphene at V_{DS} = 0.5 V. (c) I_{DS}-V_{DS} characteristics of monolayer MoS_2 at different back gate biases. Inset: transfer curve of MoS_2. (d) I_{DS}-V_{DS} characteristics and (e) transfer curves of MoS_2/graphene with different irradiation doses. (f) Dependence of I_{On}/I_{Off} ratio on the irradiation doses.

transfer (p-type doping) layer but also as an electron blocking layer that prevents MoS_2 from being affected by the substrate.

Besides optical properties, electrical properties of MoS_2/graphene heterostructures under electron irradiation are also intriguing. Recently, many studies have been reported on the electrical transport properties of MoS_2 [47,48], graphene [49,50], and their heterostructures [51]. Graphene is also found to be ideal electrodes for ohmic contacts with 2D semiconductors such as MoS_2 [52]. However, there is still lack of analysis of the effect of irradiation on the electrical properties of MoS_2/graphene heterostructure. As shown in Figs 1b and 5a, we built three terminals, field-effect devices with the horizontal MoS_2/graphene heterostructure as the channel, SiO_2 (300 nm thick) as the dielectric layer, and Si as the back gate. One electrode was fabricated on MoS_2 and another one on graphene (Fig. 5a), such that the electrical properties of MoS_2, graphene, and MoS_2/graphene heterostructure can be measured separately. The metal electrodes consisting of Cr/Au (5 nm/ 50 nm) were fabricated by standard electron beam lithography followed by electron beam evaporation.

Before irradiation, we first measured the electrical transport properties of pristine graphene (Fig. 5b) and monolayer MoS_2 (Fig. 5c) respectively in the ambient environment. Fig. 5b shows the output characteristics (I_{DS}-V_{DS}) of graphene at various back gate voltages (V_G), suggesting a p-type behavior and perfect ohmic contacts that are typical for metal/zero-band semiconductor junctions [53]. The transfer curve (I_{DS}-V_G) of graphene at a drain-source bias of V_{DS} = 0.5 V shows the Dirac point of graphene at approximately 55 V (inset of Fig. 5b), also confirming the highly p-type doping of graphene. Fig. 5c shows the I_{DS}-V_{DS} curves of the monolayer MoS_2. The almost symmetric and linear I_{DS}-V_{DS} curves can be explained by the formation of Schottky diodes in the metal-semiconductor-metal (M-S-M) structure with similar Schottky barrier heights at both ends [41]. The inset of Fig. 5c shows the transfer characteristics (I_{DS}-V_G) of MoS_2 at V_{DS} = 0.5 V, which is the characteristic of a typical n-type channel.

We further measured the electrical properties of MoS_2/graphene heterostructure after electron irradiation treatment. The output characteristics (I_{DS}-V_{DS}) of MoS_2/graphene is plotted in Fig. 5d, where the back-gate voltage is fixed at V_G = 60 V. The electrical conductance of the MoS_2/graphene heterostructure gradually reduces with the increase of the irradiation dose. This degradation should result from the irradiation-induced defects that increase the scattering probabilities of carriers and reduces the mobility of either MoS_2 or graphene. Similar

degradation can also be found in the transfer characteristics (I_{DS}-V_G) of the MoS_2/graphene FET (Fig. 5e). The I_{On}/I_{Off} ratio reduces gradually from ~1.7×10^4 for the pristine sample to ~1.3×10^3 at the dose of 2.7×10^{15} electrons cm^{-2}. It indicates that the MoS_2/graphene FETs still keep a reasonable On/Off ratio after a high dose of irradiation (Fig. 5f).

In summary, we bombarded the samples with a homemade electron gun, and systematically investigated the effect of electron irradiation on the optical and electrical properties of the monolayer MoS_2, graphene and their heterostructure. Under the same irradiation condition, the PL peak of MoS_2/graphene is more robust than that of monolayer MoS_2, which is attributed to the blocking effect of graphene that prevents MoS_2 from being affected by the substrate. Our studies on the effect of electron irradiation can pave the way toward developing irradiation-resistant semiconductor devices based on 2D heterostructures. The findings illuminate possibilities to engineer a wider range of 2D heterostructures by versatile approaches of particle irradiations (e.g., high-energy He^{2+} that has a larger penetration depth than electrons) in the future work.

Received 27 February 2018; accepted 21 March 2018; published online 17 April 2018

1 Novoselov KS, Geim AK, Morozov SV, *et al.* Electric field effect in atomically thin carbon films. Science, 2004, 306: 666–669
2 Jin W, Yeh PC, Zaki N, *et al.* Direct measurement of the thickness-dependent electronic band structure of MoS_2 using angle-resolved photoemission spectroscopy. Phys Rev Lett, 2013, 111: 106801
3 Mak KF, Lee C, Hone J, *et al.* Atomically thin MoS_2: a new direct-gap semiconductor. Phys Rev Lett, 2010, 105: 136805
4 Splendiani A, Sun L, Zhang Y, *et al.* Emerging photoluminescence in monolayer MoS_2. Nano Lett, 2010, 10: 1271–1275
5 Zhang Y, Chang TR, Zhou B, *et al.* Direct observation of the transition from indirect to direct bandgap in atomically thin epitaxial $MoSe_2$. Nat Nanotechnol, 2014, 9: 111–115
6 Wu B, Yin J, Ding Y, *et al.* A new two-dimensional $TeSe_2$ semiconductor: indirect to direct band-gap transitions. Sci China Mater, 2017, 60: 747–754
7 Lopez-Sanchez O, Lembke D, Kayci M, *et al.* Ultrasensitive photodetectors based on monolayer MoS_2. Nat Nanotechnol, 2013, 8: 497–501
8 Zhang Y, Tang TT, Girit C, *et al.* Direct observation of a widely tunable bandgap in bilayer graphene. Nature, 2009, 459: 820–823
9 Yang X, Li Q, Hu G, *et al.* Controlled synthesis of high-quality crystals of monolayer MoS_2 for nanoelectronic device application. Sci China Mater, 2016, 59: 182–190
10 Lin Z, Yin A, Mao J, *et al.* Scalable solution-phase epitaxial growth of symmetry-mismatched heterostructures on two-dimensional crystal soft template. Sci Adv, 2016, 2: e1600993–e1600993
11 Yu WJ, Liu Y, Zhou H, *et al.* Highly efficient gate-tunable photocurrent generation in vertical heterostructures of layered materials. Nat Nanotechnol, 2013, 8: 952–958
12 Yang T, Zheng B, Wang Z, *et al.* Van der Waals epitaxial growth and optoelectronics of large-scale WSe_2/SnS_2 vertical bilayer p–n junctions. Nat Commun, 2017, 8: 1906
13 Britnell L, Ribeiro RM, Eckmann A, *et al.* Strong light-matter interactions in heterostructures of atomically thin films. Science, 2013, 340: 1311–1314
14 Tongay S, Fan W, Kang J, *et al.* Tuning interlayer coupling in large-area heterostructures with CVD-grown MoS_2 and WS_2 monolayers. Nano Lett, 2014, 14: 3185–3190
15 Li B, Huang L, Zhong M, *et al.* Direct vapor phase growth and optoelectronic application of large band offset SnS_2/MoS_2 vertical bilayer heterostructures with high lattice mismatch. Adv Electron Mater, 2016, 2: 1600298
16 Liu J, Cao H, Jiang B, *et al.* Newborn 2D materials for flexible energy conversion and storage. Sci China Mater, 2016, 59: 459–474
17 Huo N, Tongay S, Guo W, *et al.* Novel optical and electrical transport properties in atomically thin WSe_2/MoS_2 p-n heterostructures. Adv Electron Mater, 2015, 1: 1400066
18 Wang X, Huang L, Peng Y, *et al.* Enhanced rectification, transport property and photocurrent generation of multilayer $ReSe_2/MoS_2$ p–n heterojunctions. Nano Res, 2016, 9: 507–516
19 Yuan H, Liu X, Afshinmanesh F, *et al.* Polarization-sensitive broadband photodetector using a black phosphorus vertical p–n junction. Nat Nanotechnol, 2015, 10: 707–713
20 Liu Z, Zhang Y, Zhao H, *et al.* Constructing monodispersed $MoSe_2$ anchored on graphene: a superior nanomaterial for sodium storage. Sci China Mater, 2017, 60: 167–177
21 Li Y, Huang L, Li B, *et al.* Co-nucleus 1D/2D heterostructures with Bi_2S_3 nanowire and MoS_2 monolayer: one-step growth and defect-induced formation mechanism. ACS Nano, 2016, 10: 8938–8946
22 López-Polín G, Gómez-Navarro C, Parente V, *et al.* Increasing the elastic modulus of graphene by controlled defect creation. Nat Phys, 2015, 11: 26–31
23 Bertolazzi S, Bonacchi S, Nan G, *et al.* Engineering chemically active defects in monolayer MoS_2 transistors *via* ion-beam irradiation and their healing *via* vapor deposition of alkanethiols. Adv Mater, 2017, 29: 1606760
24 Parkin WM, Balan A, Liang L, *et al.* Raman shifts in electron-irradiated monolayer MoS_2. ACS Nano, 2016, 10: 4134–4142
25 Komsa HP, Kotakoski J, Kurasch S, *et al.* Two-dimensional transition metal dichalcogenides under electron irradiation: defect production and doping. Phys Rev Lett, 2012, 109: 035503
26 Zhou Y, Jadwiszczak J, Keane D, *et al.* Programmable graphene doping *via* electron beam irradiation. Nanoscale, 2017, 9: 8657–8664
27 Fox DS, Zhou Y, Maguire P, *et al.* Nanopatterning and electrical tuning of MoS_2 layers with a subnanometer helium ion beam. Nano Lett, 2015, 15: 5307–5313
28 Liu K, Hsin CL, Fu D, *et al.* Self-passivation of defects: effects of high-energy particle irradiation on the elastic modulus of multilayer graphene. Adv Mater, 2015, 27: 6841–6847
29 Tongay S, Suh J, Ataca C, *et al.* Defects activated photoluminescence in two-dimensional semiconductors: interplay between bound, charged and free excitons. Sci Rep, 2013, 3: 2657
30 Tan Y, Liu X, He Z, *et al.* Tuning of interlayer coupling in large-area graphene/WSe_2 van der Waals heterostructure *via* ion irradiation: optical evidences and photonic applications. ACS Photonics, 2017, 4: 1531–1538
31 Nan H, Wang Z, Wang W, *et al.* Strong photoluminescence en-

hancement of MoS_2 through defect engineering and oxygen bonding. ACS Nano, 2014, 8: 5738–5745
32 Nan H, Wu Z, Jiang J, *et al.* Improving the electrical performance of MoS_2 by mild oxygen plasma treatment. J Phys D-Appl Phys, 2017, 50: 154001
33 Zandiatashbar A, Lee GH, An SJ, *et al.* Effect of defects on the intrinsic strength and stiffness of graphene. Nat Commun, 2014, 5
34 Carpenter C, Maroudas D, Ramasubramaniam A. Mechanical properties of irradiated single-layer graphene. Appl Phys Lett, 2013, 103: 013102
35 Weerasinghe A, Ramasubramaniam A, Maroudas D. Thermal conductivity of electron-irradiated graphene. Appl Phys Lett, 2017, 111: 163101
36 Krasheninnikov AV, Banhart F. Engineering of nanostructured carbon materials with electron or ion beams. Nat Mater, 2007, 6: 723–733
37 Yu Y, Yu Y, Xu C, *et al.* Engineering substrate interactions for high luminescence efficiency of transition-metal dichalcogenide monolayers. Adv Funct Mater, 2016, 26: 4733–4739
38 Mak KF, He K, Lee C, *et al.* Tightly bound trions in monolayer MoS_2. Nat Mater, 2013, 12: 207–211
39 Cançado LG, Jorio A, Ferreira EHM, *et al.* Quantifying defects in graphene *via* Raman spectroscopy at different excitation energies. Nano Lett, 2011, 11: 3190–3196
40 Pimenta MA, Dresselhaus G, Dresselhaus MS, *et al.* Studying disorder in graphite-based systems by Raman spectroscopy. Phys Chem Chem Phys, 2007, 9: 1276–1290
41 Dong H, Liu H. Elastic properties of VO_2 from first-principles calculation. Solid State Commun, 2013, 167: 1–4
42 Liu M, Shi J, Li Y, *et al.* Temperature-triggered sulfur vacancy evolution in monolayer MoS_2/graphene heterostructures. Small, 2017, 13: 1602967
43 Tongay S, Zhou J, Ataca C, *et al.* Broad-range modulation of light emission in two-dimensional semiconductors by molecular physisorption gating. Nano Lett, 2013, 13: 2831–2836
44 Sun Y, Wang R, Liu K. Substrate induced changes in atomically thin 2-dimensional semiconductors: Fundamentals, engineering, and applications. Appl Phys Rev, 2017, 4: 011301
45 Yuan ZQ, Hou JW, Liu K. Interfacing 2D semiconductors with functional oxides: Fundamentals, properties, and applications. Crystals, 2017, 7: 265
46 Hou J, Wang X, Fu D, *et al.* Modulating photoluminescence of monolayer molybdenum disulfide by metal-insulator phase transition in active substrates. Small, 2016, 12: 3976–3984
47 Late DJ, Liu B, Matte HSSR, *et al.* Hysteresis in single-layer MoS_2 field effect transistors. ACS Nano, 2012, 6: 5635–5641
48 Radisavljevic B, Kis A. Mobility engineering and a metal–insulator transition in monolayer MoS_2. Nat Mater, 2013, 12: 815–820
49 Castro Neto AH, Guinea F, Peres NMR, *et al.* The electronic properties of graphene. Rev Mod Phys, 2009, 81: 109–162
50 Geim AK, Novoselov KS. The rise of graphene. Nat Mater, 2007, 6: 183–191
51 Kwak JY, Hwang J, Calderon B, *et al.* Electrical characteristics of multilayer MoS_2 FET's with MoS_2/graphene heterojunction contacts. Nano Lett, 2014, 14: 4511–4516
52 Xie L, Liao M, Wang S, *et al.* Graphene-contacted ultrashort channel monolayer MoS_2 transistors. Adv Mater, 2017, 29: 1702522
53 Kim BJ, Jang H, Lee SK, *et al.* High-performance flexible graphene field effect transistors with ion gel gate dielectrics. Nano Lett, 2010, 10: 3464–3466

Acknowledgements This work was supported by the National Natural Science Foundation of China (11774191, 51727805, and 51672152), the Open Research Fund Program of the State Key Laboratory of Low-Dimensional Quantum Physics (KF201603), and the Thousand Youth Talents Program of China.

Author contributions Liu K proposed and designed the project. Hong S, Hou J, Wang B and Sun Y fabricated the samples and devices. Hong S, Zhou D and Liu P performed the irradiation experiments. Hong S measured the optical and electrical properties of the samples. Liu K, Fu D and Hong S analyzed the data. Hong S, Liu K and Fu D wrote the paper. All the authors contributed to general discussions.

Conflict of interest The authors declare that they have no conflict of interest.

Supplementary information Experimental details and supporting data are available in the online version of the paper, including transfer process of monolayer MoS_2, photoluminescence (PL) and Raman spectra of MoS_2 and graphene/MoS_2 under electron beam irradiation, X-ray photoelectron spectroscopy (XPS) spectra of monolayer MoS_2, and KPFM results of monolayer MoS_2 and MoS_2/graphene.

Shengzhe Hong obtained his bachelor's degree at Taipei University of Technology in 2015, and is now a postgraduate student at Tsinghua University. His research interests are focused on the effects of electron-beam irradiation on two-dimensional materials and heterostructures.

Kai Liu obtained his PhD degree from Tsinghua University in 2008. He joined Tsinghua University as an associtate professor in 2015 after a period of postdoctoral research at the Lawrence-Berkeley National Lab, USA. His current research is focused on syntheses and applications of low-dimensional materials and their composites or heterostructures.

二硫化钼/石墨烯异质结在电子束辐照轰击下发光能量的鲁棒特性

洪聖哲[1†], 傅德颐[2†], 侯纪伟[1], 周段亮[3], 王博伦[1], 孙雨飞[1], 柳鹏[3], 刘锴[1*]

摘要 在许多恶劣的工作环境中, 器件难免会曝露在电子束辐照下. 对于单原子层厚度的二维材料而言, 电子束辐照经常会造成其本征性能的衰减. 如何避开这一影响对于多功能化的二维异质结器件来讲至关重要. 然而, 电子束辐照对于二维异质结的影响至今仍缺乏充分深入的研究. 本工作发现利用异质结的堆垛可以阻碍单层二硫化钼(MoS_2)由于电子束辐照带来的性能衰退. 通过在MoS_2与基底之间插入单层石墨烯, 在同样剂量的电子束辐照轰击下, 异质结区域的光致发光强度始终大于纯单层MoS_2; 而且与纯单层区域明显的发光能量变化相比, MoS_2/石墨烯异质结区域的发光能量具有更佳的稳定性. 这一现象归因于石墨烯的阻隔效应: 由于单层石墨烯的存在抑制了基板对MoS_2的影响. 此外, 我们也系统地揭示了电子束辐照对MoS_2/石墨烯异质结拉曼光谱及电学传输特性的影响. 本工作不仅有助于加深人们对二维异质结辐照效应的认知, 同时也为新型抗辐射器件的设计开辟了新的途径.

